Science Advances
AAAS

Supplementary Materials for

Unmasking of the von Willebrand A-domain surface adhesin CglB at bacterial focal adhesions mediates myxobacterial gliding motility

Salim T. Islam *et al.*

Corresponding author: Tâm Mignot, tmignot@imm.cnrs.fr; Salim T. Islam, salim.islam@inrs.ca

Sci. Adv. **9**, eabq0619 (2023)
DOI: 10.1126/sciadv.abq0619

This PDF file includes:

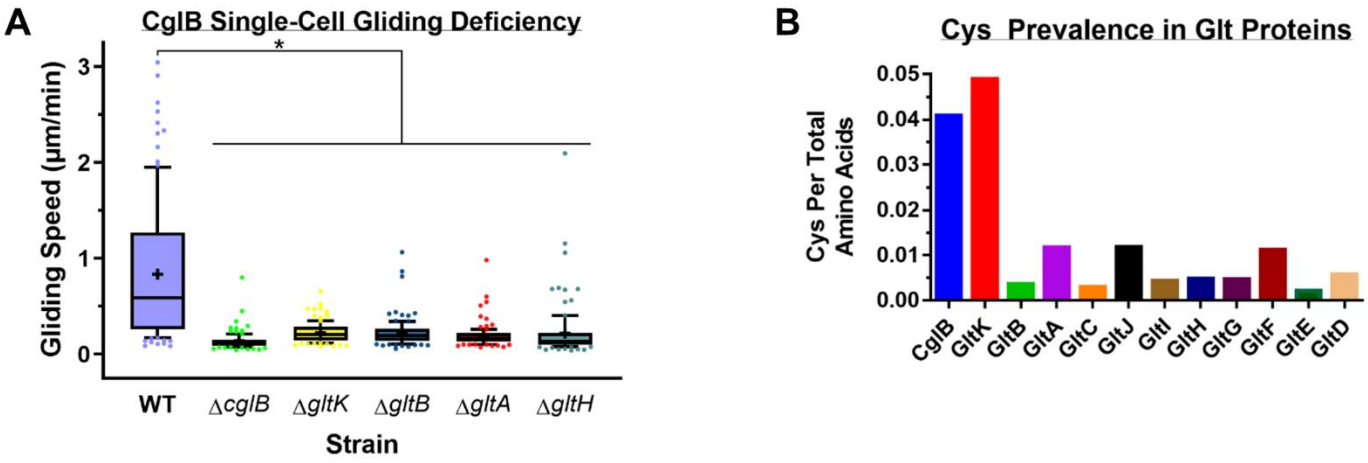

Fig. S1. CglB gliding motility importance and protein characteristics. A) Single-cell gliding speeds for *M. xanthus* OM-module mutant strains (n = 100 cells) on CYE hard (1.5%) agar. The lower and upper boundaries of the boxes correspond to the 25th and 75th percentiles, respectively. The median (line through centre of boxplot) and mean (+) of each dataset are indicated. Lower and upper whiskers represent the 10th and 90th percentiles, respectively; data points above and below the whiskers are drawn as individual points. Asterisks denote datasets displaying statistically significant differences in dataset distributions ($P < 0.0001$) relative to WT, as determined via unpaired two-tailed Mann-Whitney tests. **B)** Ratio of number of Cys residues per gliding motility-complex protein, divided by the total number of amino acids in that protein.

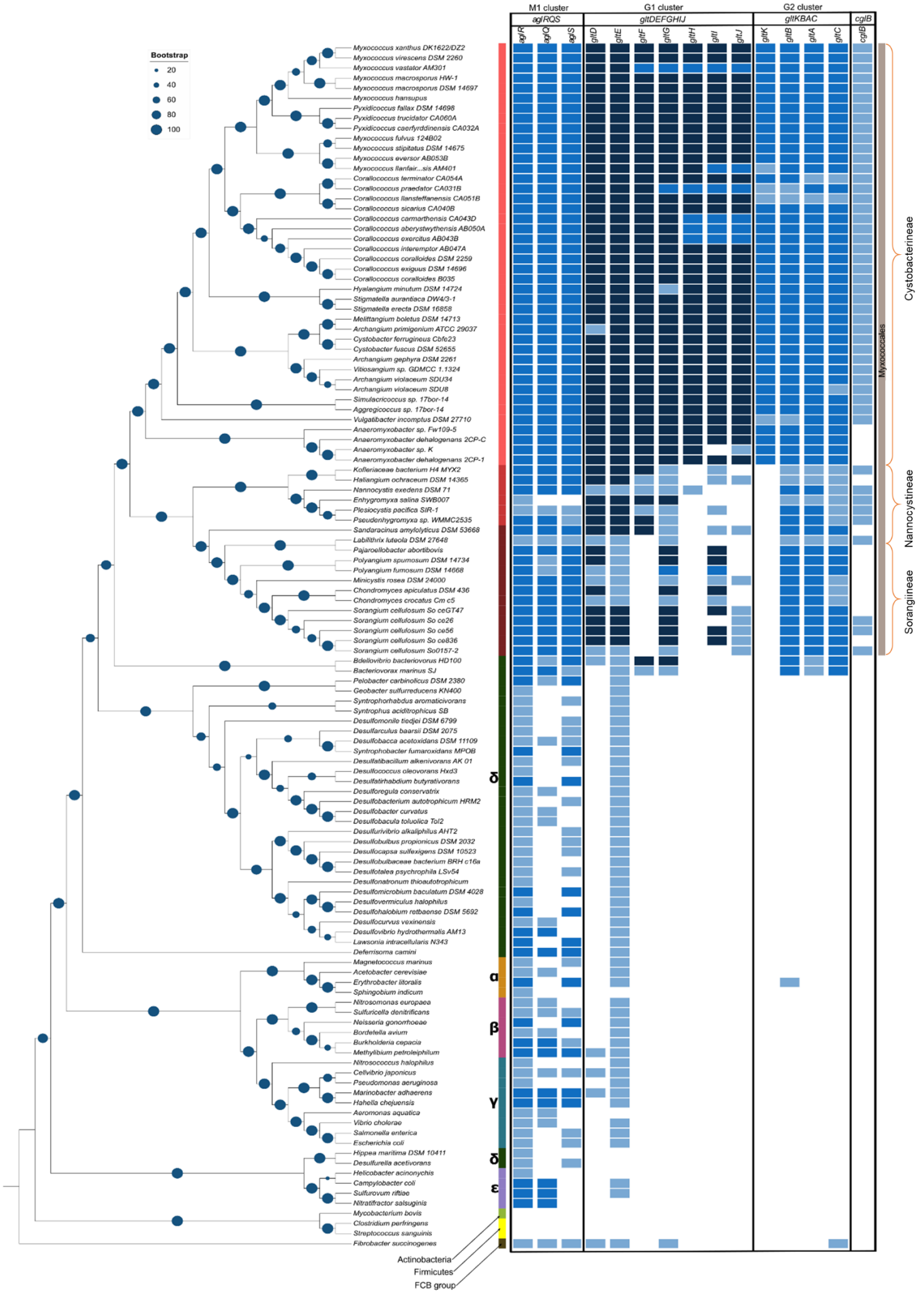
M1 cluster
G1 cluster
G2 cluster
aglRQS
gltDEFGHIJ
gltKBAC
cglB
aglR
aglQ
aglS
gltD
gltE
gltF
gltG
gltH
gltI
gltJ
gltK
gltB
gltA
gltC
cglB
Bootstrap
20
40
60
80
100
Myxococcus xanthus DK1622/DZ2
Myxococcus virescens DSM 2260
Myxococcus vastator AM301
Myxococcus macrosporus HW-1
Myxococcus macrosporus DSM 14697
Myxococcus hansupus
Pyxidicoccus fallax DSM 14698
Pyxidicoccus trucidator CA060A
Pyxidicoccus caerfyrddinensis CA032A
Myxococcus fulvus 124B02
Myxococcus stipitatus DSM 14675
Myxococcus eversor AB053B
Myxococcus llanfair...sis AM401
Corallococcus terminator CA054A
Corallococcus praedator CA031B
Corallococcus llansteffanensis CA051B
Corallococcus sicarius CA040B
Corallococcus carmarthensis CA043D
Corallococcus aberystwythensis AB050A
Corallococcus exercitus AB043B
Corallococcus interemptor AB047A
Corallococcus coralloides DSM 2259
Corallococcus exiguus DSM 14696
Corallococcus coralloides B035
Hyalangium minutum DSM 14724
Stigmatella aurantiaca DW4/3-1
Stigmatella erecta DSM 16858
Melittangium boletus DSM 14713
Archangium primigenium ATCC 29037
Cystobacter ferrugineus Cbfe23
Cystobacter fuscus DSM 52655
Archangium gephyra DSM 2261
Vitiosangium sp. GDMCC 1.1324
Archangium violaceum SDU34
Archangium violaceum SDU8
Simulacricoccus sp. 17bor-14
Aggregicoccus sp. 17bor-14
Vulgatibacter incomptus DSM 27710
Anaeromyxobacter sp. Fw109-5
Anaeromyxobacter dehalogenans 2CP-C
Anaeromyxobacter sp. K
Anaeromyxobacter dehalogenans 2CP-1
Kofleriaceae bacterium H4 MYX2
Haliangium ochraceum DSM 14365
Nannocystis exedens DSM 71
Enhygromyxa salina SWB007
Plesiocystis pacifica SIR-1
Pseudenhygromyxa sp. WMMC2535
Sandaracinus amylolyticus DSM 53668
Labilithrix luteola DSM 27648
Pajaroellobacter abortibovis
Polyangium spumosum DSM 14734
Polyangium fumosum DSM 14668
Minicystis rosea DSM 24000
Chondromyces apiculatus DSM 436
Chondromyces crocatus Cm c5
Sorangium cellulosum So ceGT47
Sorangium cellulosum So ce26
Sorangium cellulosum So ce56
Sorangium cellulosum So ce836
Sorangium cellulosum So0157-2
Bdellovibrio bacteriovorus HD100
Bacteriovorax marinus SJ
Pelobacter carbinolicus DSM 2380
Geobacter sulfurreducens KN400
Syntrophorhabdus aromaticivorans
Syntrophus aciditrophicus SB
Desulfomonile tiedjei DSM 6799
Desulfarculus baarsii DSM 2075
Desulfobacca acetoxidans DSM 11109
Syntrophobacter fumaroxidans MPOB
Desulfatibacillum alkenivorans AK 01
Desulfococcus oleovorans Hxd3
Desulfatirhabdium butyrativorans
Desulforegula conservatrix
Desulfobacterium autotrophicum HRM2
Desulfobacter curvatus
Desulfobacula toluolica Tol2
Desulfurivibrio alkaliphilus AHT2
Desulfobulbus propionicus DSM 2032
Desulfocapsa sulfexigens DSM 10523
Desulfobulbaceae bacterium BRH c16a
Desulfotalea psychrophila LSv54
Desulfonatronum thioautotrophicum
Desulfomicrobium baculatum DSM 4028
Desulfovermiculus halophilus
Desulfohalobium retbaense DSM 5692
Desulfocurvus vexinensis
Desulfovibrio hydrothermalis AM13
Lawsonia intracellularis N343
Deferrisoma camini
Magnetococcus marinus
Acetobacter cerevisiae
Erythrobacter litoralis
Sphingobium indicum
Nitrosomonas europaea
Sulfuricella denitrificans
Neisseria gonorrhoeae
Bordetella avium
Burkholderia cepacia
Methylibium petroleiphilum
Nitrosococcus halophilus
Cellvibrio japonicus
Pseudomonas aeruginosa
Marinobacter adhaerens
Hahella chejuensis
Aeromonas aquatica
Vibrio cholerae
Salmonella enterica
Escherichia coli
Hippea maritima DSM 10411
Desulfurella acetivorans
Helicobacter acinonychis
Campylobacter coli
Sulfurovum riftiae
Nitratifractor salsuginis
Mycobacterium bovis
Clostridium perfringens
Streptococcus sanguinis
Fibrobacter succinogenes
δ
α
β
γ
δ
ε
Actinobacteria
Firmicutes
FCB group
Myxococcales
Cystobacterineae
Nannocystineae
Sorangiineae

Fig. S2. CglB co-occurrence and gene synteny in bacteria. Taxonomic distribution and co-occurrence of *agl* and *glt* genes in bacteria. Bootstrap values at each node are indicated as shown in the side legends. Colour of gene hit indicates synteny with the G1 *gltDEFGHIJ* (dark blue) or G2 *gltKBAC (*blue) gene clusters or lack thereof (light blue), respectively. Herein, synteny denotes a minimum of three genes in the vicinity of each other.

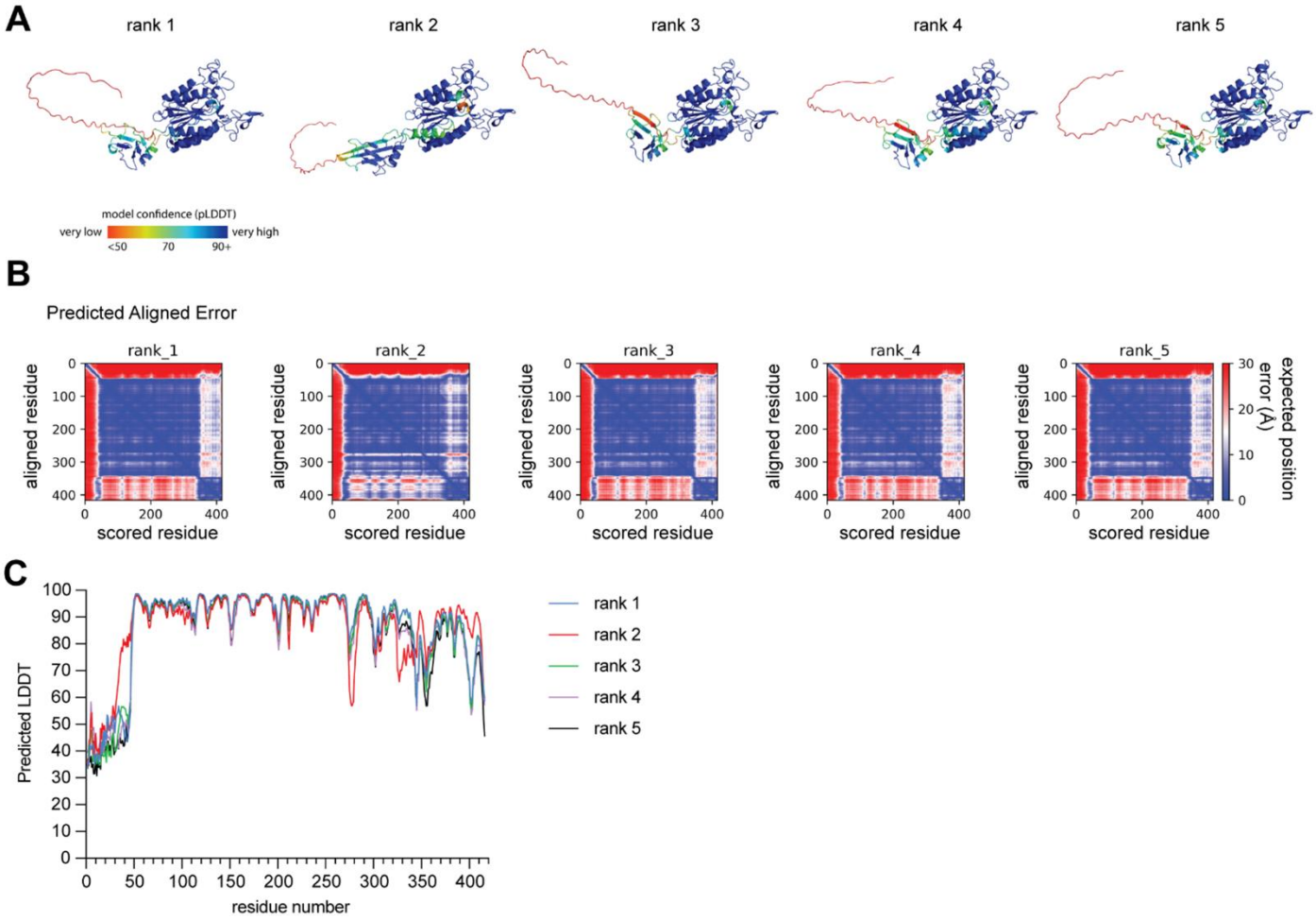

Fig. S3. AlphaFold prediction quality for the CglB tertiary-structure model. (A) AlphaFold CglB models ranked from 1 to 5. Per-residue confidence scores (pLDDT: predicted local-distance different test) are directly reported on the 3D structure of CglB (with the range of possible values from 50 [*red*] to 90 [*blue*]). **(B)** Corresponding predicted aligned error for each ranked model. **(C)** Plot showing the corresponding pLDDT scores per residue for each ranked model.

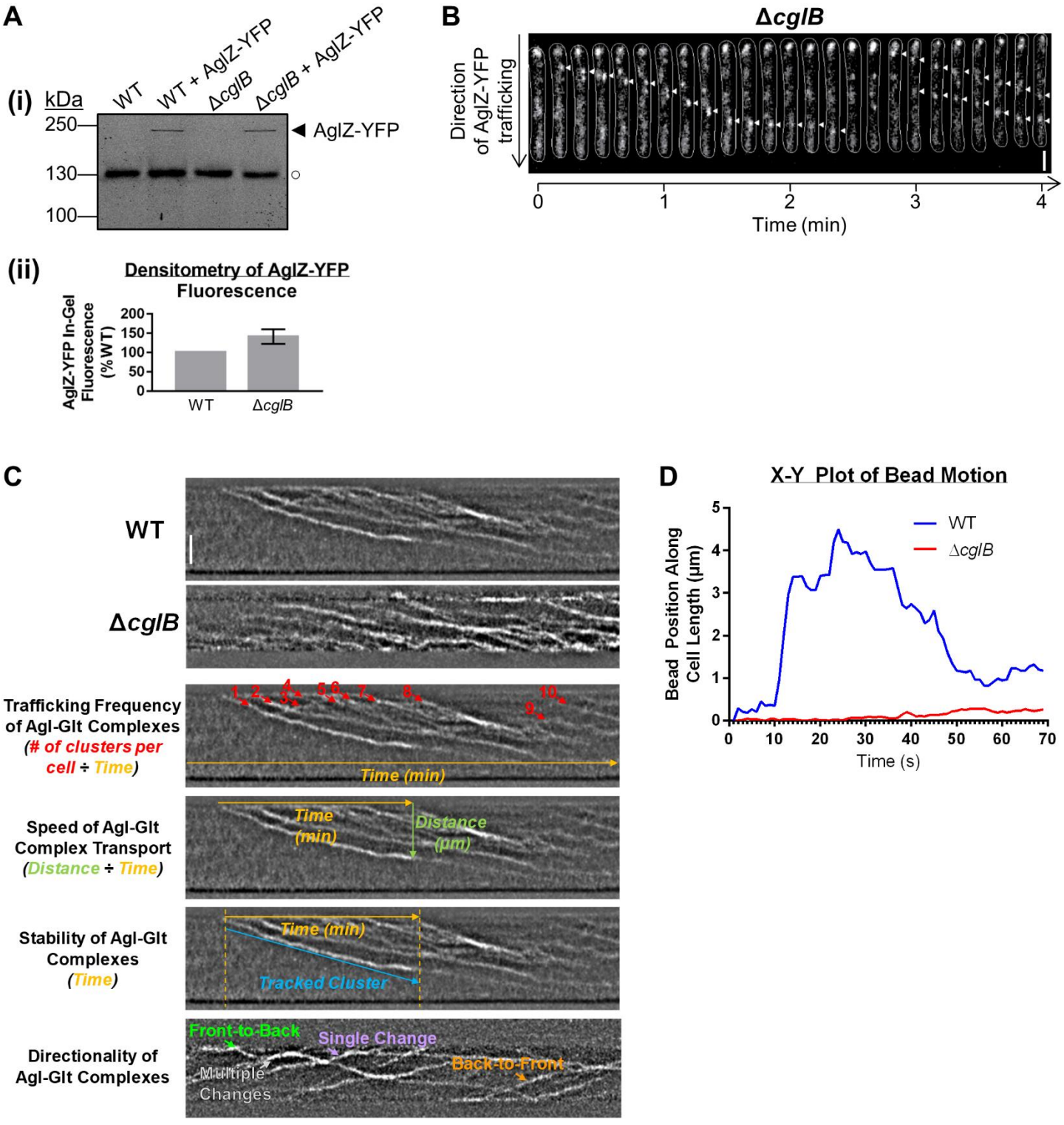
A
(i)
kDa
WT
WT + AglZ-YFP
ΔcglB
ΔcglB + AglZ-YFP
250
130
100
AglZ-YFP
(ii)
Densitometry of AglZ-YFP Fluorescence
AglZ-YFP In-Gel Fluorescence (% WT)
200
150
100
50
0
WT
ΔcglB
B
ΔcglB
Direction of AglZ-YFP trafficking
0
1
2
3
4
Time (min)
C
WT
ΔcglB
Trafficking Frequency of Agl-Glt Complexes
(# of clusters per cell ÷ Time)
1
2
3
4
5
6
7
8
9
10
Time (min)
Speed of Agl-Glt Complex Transport
(Distance ÷ Time)
Time (min)
Distance (μm)
Stability of Agl-Glt Complexes
(Time)
Time (min)
Tracked Cluster
Directionality of Agl-Glt Complexes
Front-to-Back
Single Change
Back-to-Front
Multiple Changes
D
X-Y Plot of Bead Motion
Bead Position Along Cell Length (μm)
5
4
3
2
1
0
WT
ΔcglB
0
10
20
30
40
50
60
70
Time (s)

Fig. S4. Role of CglB in Agl–Glt complex localization and directed surface transport. (A) In-gel fluorescence (i) scan and (ii) densitometry analysis of AglZ-YFP levels in WT vs. Δ*cglB* crude-cell lysates resolved via SDS-PAGE. Fluorescence levels were analyzed across six biological replicates and are displayed +/− SEM. Despite a higher mean value for AglZ-YFP levels in Δ*cglB* cells than in WT cells, this difference was not statistically significant, as determined via Wilcoxon signed-rank test performed relative to "100" (*P = 0.0938*). **(B)** Fluorescence microscopy time-course montage of *M. xanthus* Δ*cglB* (on hard agar) expressing AglZ-YFP, clusters of which are indicated (*white arrowheads*). Images were acquired at 10 s intervals. Scale bar: 2 μm. **(C)** Kymograph of AglZ-YFP localization in *M. xanthus* cells on chitosan-coated PDMS microfluidic chambers via TIRFM. Arrows in *orange* denote sequential kymograph slices over time. Arrows in *cyan* indicate positions of trafficked Agl–Glt clusters in the cell. The manners in which various fluorescent-cluster tracking data (see Fig. 5C-F) were obtained have been indicated in the example images. Scale bar: 3 μm **(D)** Representative time course of polystyrene bead position tracking along the length of a cell (see Fig. 5H).

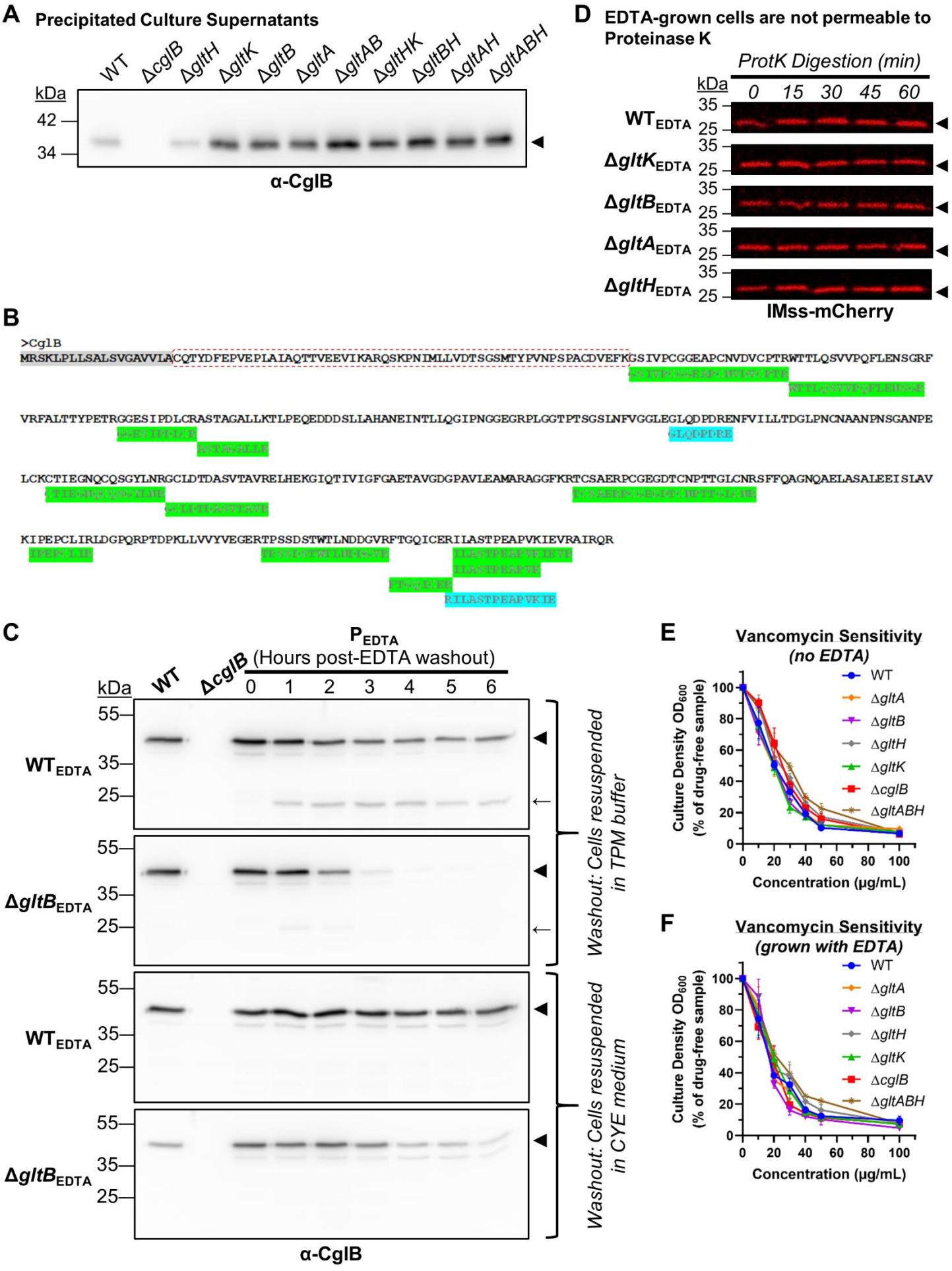
A
Precipitated Culture Supernatants
WT
ΔcglB
ΔgltH
ΔgltK
ΔgltB
ΔgltA
ΔgltAB
ΔgltHK
ΔgltBH
ΔgltAH
ΔgltABH
kDa
42
34
α-CglB
D
EDTA-grown cells are not permeable to Proteinase K
ProtK Digestion (min)
kDa
0 15 30 45 60
WT EDTA
ΔgltK EDTA
ΔgltB EDTA
ΔgltA EDTA
ΔgltH EDTA
35
25
IMss-mCherry
B
>CglB
MRSKLPLLSALSVGAVVLACQTYDFEPVEPLAIAQTTVEEVIKARQSKPNIMLLVDTSGSMTYPVNPSPACDVEFKGSIVPCGGEAPCNVDVCPTRWTTLQSVVPQFLENSGRF
VRFALTTYPETRGGESIPDLCRASTAGALLKTLPEQEDDDSLLAHANEINTLLQGIPNGGEGRPLGGTPTSGSLNFVGGLEGLQDPDRENFVILLTDGLPNCNAANPNSGANPE
LCKCTIEGNQCQSGYLNRGCLDTDASVTAVRELHEKGIQTIVIGFGAETAVGDGPAVLEAMARAGGFKRTCSAERPCGEGDTCNPTTGLCNRSFFQAGNQAELASALEEISLAV
KIPEPCLIRLDGPQRPTDPKLLVVYVEGERTPSSDSTWTLNDDGVRFTGQICERILASTPEAPVKIEVRAIRQR
C
P EDTA
(Hours post-EDTA washout)
kDa
WT
ΔcglB
0 1 2 3 4 5 6
55
35
25
WT EDTA
ΔgltB EDTA
Washout: Cells resuspended in TPM buffer
Washout: Cells resuspended in CYE medium
α-CglB
E
Vancomycin Sensitivity
(no EDTA)
Culture Density OD600
(% of drug-free sample)
Concentration (μg/mL)
WT
ΔgltA
ΔgltB
ΔgltH
ΔgltK
ΔcglB
ΔgltABH
F
Vancomycin Sensitivity
(grown with EDTA)
Culture Density OD600
(% of drug-free sample)
Concentration (μg/mL)

Fig. S5. Possibility of post-translational processing of CglB. (A) Precipitated soluble supernatant samples from Δ*glt* mutants that exhibit depleted levels of cell-associated CglB. Equivalent supernatant volumes from different strains were filtered through a 0.2 µm filter, sedimented in an ultracentrifuge (120 000 × *g*, 85 min, 4 ºC), then treated with TCA to precipitate all remaining soluble proteins. Legend: ◄, truncated CglB. **(B)** Peptides identified via trypsin/V8 digestion and mass spectrometric analysis of immunoprecipitated CglB from Δ*gltB* culture supernatant. Legend: *grey*, predicted signal peptide; *green*, trypsin-derived peptide; *cyan*, V8-derived peptide; *red box*, N-terminal tract of CglB unaccounted for by mass spectrometry. **(C)** α-CglB Western immunoblot demonstrating the resumption of CglB release from EDTA-grown cells upon transfer to an EDTA-free minimal buffer (TPM) or rich medium (CYE). Legend: ◄, full-length CglB; ←, CglB degradation band; P_{EDTA}, parent strain (WT or Δ*gltB*) grown in the presence of EDTA. **(D)** In-gel fluorescence (following SDS-PAGE) of EDTA-grown cells treated with Proteinase K. Each strain (WT, Δ*gltK/B/A/H*) was made to express IMss-mCherry, a modified fluorescent mCherry that is expressed in the periplasm but remains tethered to the IM. Digestion aliquots were removed at 15-min intervals and heat-inactivated to stop digestion. **(E)** Vancomycin sensitivity curves for mutant strains defective for various constituents of the Glt OM platform. Strains (n = 3) were grown in CYE liquid broth with increasing concentrations of the antibiotic. **(F)** Vancomycin sensitivity curves for mutant strains defective for various constituents of the Glt OM platform. Strains (n = 3) were grown in CYE liquid broth in the presence of EDTA (1 mM) with increasing concentrations of the antibiotic. For Panels E and F, mean values for each mutant strain were compared to that of WT at each concentration using two-way ANOVA and Dunnett's multiple comparisons test, with a single pooled variance. No statistically significant differences were detected ($P > 0.05$) at any vancomycin concentration.

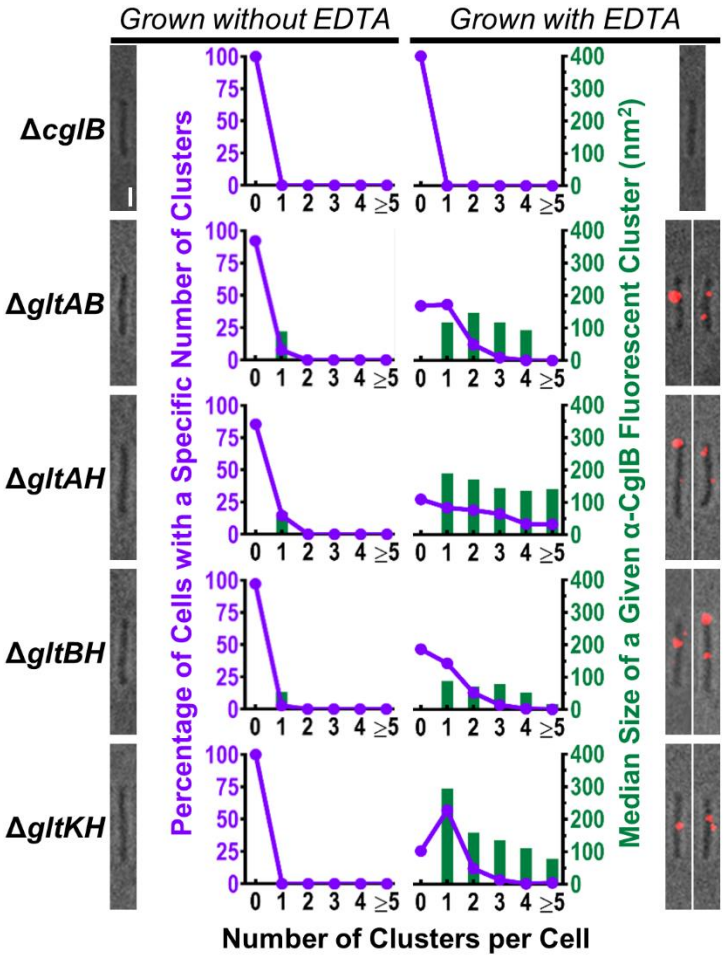

Fig. S6. CglB localizes to the cell surface despite Glt OM-platform deficiencies. Fluorescence micrographs of live immunolabelled Δ*cglB*, Δ*gltAB*, Δ*gltAH*, Δ*gltBH*, and Δ*gltHK* cells grown with(out) EDTA (labelled with α-CglB 1º antibody, followed by goat α-rabbit 2º antibody conjugated to AlexaFluor647) on agar pads at 32 ºC. Representative images are provided for cluster labelling patterns observed on ~20% or more of analyzed cells for a given strain and treatment. Scale bar: 1 µm. For each strain grown with(out) EDTA, the number of fluorescent clusters detected per cell was counted (X-axis) and compared against the proportion of cells with such a labelling phenotype (purple left-side Y-axis). The size of each cluster was also measured, with the median area (dark green right-side Y-axis) given for each labelling phenotype. The number of cells analyzed for each treatment is as follows (−/+ EDTA): Δ*cglB* 361/373, Δ*gltAB* 319/471, Δ*gltAH* 534/262, Δ*gltBH* 647/335, Δ*gltKH* 478/394.

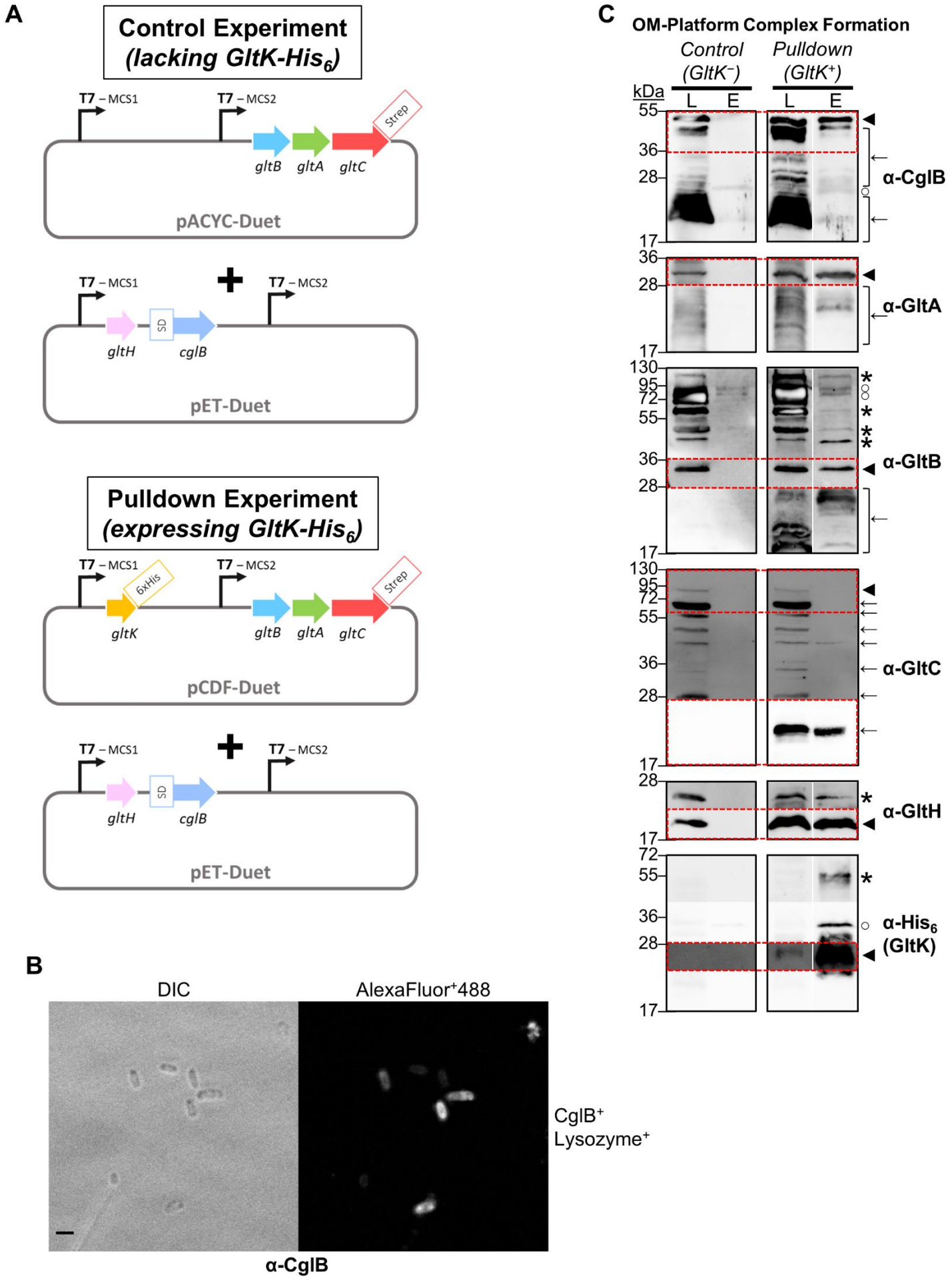
A
Control Experiment
(lacking GltK-His6)
T7 – MCS1
T7 – MCS2
Strep
gltB
gltA
gltC
pACYC-Duet
T7 – MCS1
T7 – MCS2
SD
gltH
cglB
pET-Duet
Pulldown Experiment
(expressing GltK-His6)
T7 – MCS1
6xHis
T7 – MCS2
Strep
gltK
gltB
gltA
gltC
pCDF-Duet
T7 – MCS1
T7 – MCS2
SD
gltH
cglB
pET-Duet
B
DIC
AlexaFluor+488
CglB+
Lysozyme+
α-CglB
C
OM-Platform Complex Formation
Control
(GltK−)
Pulldown
(GltK+)
kDa
L
E
L
E
55
36
28
17
α-CglB
α-GltA
130
95
72
55
36
28
17
α-GltB
α-GltC
α-GltH
α-His6
(GltK)

Fig. S7. Heterologous expression and co-purification of the Glt OM complex with CglB. **(A)** Plasmids for the expression of the OM-platform proteins and CglB in *E. coli* BL21(DE3). Different combinations of plasmids were designed for the pulldown assay (pCDF-Duet and pET-Duet) and the negative control (pACYC-Duet and pET-Duet). A C-terminally StrepII-tagged GltC, GltB and A were cloned into MSC2 of pCDF-Duet and pACYC-Duet vector whereas a C-terminally His_6-tagged GltK was cloned into the MSC1 of pCDF-Duet. The *cglB* and *gltH* sequences were cloned in tandem into pET-Duet MSC1 with an additional Shine Dalgarno (SD). **(B)** Fluorescence micrographs of *E. coli* BL21(DE3) cells immunolabelled with α-CglB 1º antibody, followed by goat α-rabbit 2º antibody conjugated to AlexaFluor Plus 488 ($AF^{+}488$). Cells had been transformed with the following plasmids: "pCDF-Duet-$GltK^{6H}$+$GltBAC^{S}$ & pET-Duet-GltH-CglB" (for co-expression of GltA, GltB, GltC-StrepII, GltK-His_6, GltH, and CglB). Cells were induced overnight with 1.0 mM IPTG, fixed with paraformaldehyde, treated with lysozyme, then immunolabelled. Scale bar: 2 μm. **(C)** Western immunoblotting of purified OM-platform proteins from the pulldown assay (*right-side panels*) or negative control (*left-side panels*) using α-CglB, α-GltA, α-GltB, α-GltH, α-His (GltK), and α-GltC antibodies. Calculated molecular weights for monomeric forms of each protein construct (lacking signal peptide): CglB (42.3 kDa), GltA (25.4 kDa), GltB (27.5 kDa), GltC-Strep (74.4 kDa), GltH (20.0 kDa), GltK-His_6 (17.5 kDa). Lane legend: L, column loading fraction; E, column elution fraction. Blot legend: ◄, full-length protein; *, oligomeric species of the protein of interest; ←, degradation products of the protein of interest; ○, non-specific protein band (detected in the elution fractions from both the control and pulldown samples) labelled by the respective α-CglB/α-GltB/α-His antibodies).

PDB Hit	**Name *(Species)***	**Probability**	**E-value**	**Score**	**Aligned Coils**	**Identities**	**Similarity**
1MF7_A	Integrin αM *(Homo sapiens)*	99.4%	6.4E-14	123.84	187	19%	0.191
4FX5_A	Von Willebrand factor type A *(Catenulispora acidiphila)*	99.36%	3E-13	140.21	199	19%	0.161
4OKR_A	Micronemal protein MIC2 *(Toxoplasma gondii)*	99.34	3.8E-13	127.97	180	20%	0.242
4F1J_B	TRAP *(Plasmodium falciparum)*	99.18	1.1E-11	110.16	178	17%	0.257
3TXA_A	GBS104 tip pilin (*Streptococcus agalactiae* serogroup V*)*	99.13	7.2E-12	136.34	188	17%	0.239

Table S1. HHpred fold-recognition hits in the PDB to CglB.

Strain	**Genotype/Description**	**Construction**	**Source or Reference**
DZ2	WT	Wild type	Laboratory collection
TM770	Ω*cglB*	DZ2 Ω*cglB*	This work
TM913	Δ*cglB*	DZ2 Δ*cglB*	This work
TM600	Δ*gltK*	DZ2 Δ*gltK* (pBJΔ*gltK*)	(*7*)
TM603	Δ*gltB*	DZ2 Δ*gltB* (pBJΔ*gltB*)	(*7*)
TM606	Δ*gltA*	DZ2 Δ*gltA* (pBJΔ*gltA*)	(*7*)
TM570	Δ*gltC*	DZ2 Δ*gltC* (pBJΔ*gltC*)	(*7*)
TM646	Δ*gltJ*	DZ2 Δ*gltJ*	This work
TM731	Δ*gltI*	DZ2 Δ*gltI*	This work
TM149	Δ*gltH*	DZ2 Δ*gltH* (pBJΔ*gltH*)	(*7*)
TM135	Δ*gltG*	DZ2 Δ*gltG* (pBJΔ*gltG*)	(*7*)
TM136	Δ*gltF*	DZ2 Δ*gltF* (pBJΔ*gltF*)	(*7*)
TM148	Δ*gltE*	DZ2 Δ*gltE* (pBJΔ*gltE*)	(*7*)
TM142	Δ*gltD*	DZ2 Δ*gltD* (pBJΔ*gltD*)	(*7*)
TM1157	Δ*gltK* Δ*gltH*	TM149 Δ*gltK* (pBJΔ*gltK*)	This work
TM1156	Δ*gltB* Δ*gltH*	TM149 Δ*gltB* (pBJΔ*gltB*)	This work
TM1158	Δ*gltA* Δ*gltH*	TM149 Δ*gltA* (pBJΔ*gltA*)	This work
TM1154	Δ*gltA* Δ*gltB*	DZ2 pBJΔ*gltBA*	This work
TM1397	Δ*gltA* Δ*gltB* Δ*gltH*	TM149 Δ*gltBA* (pBJΔ*gltBA*)	This work
TM829	WT + *aglZ-YFP*	DZ2 pBJ*AglZ-YFP*	(*12*)
TM1181	Δ*cglB* + *aglZ-YFP*	TM913 *aglZ-YFP* (pBJ*AglZ-YFP*)	This work
TM1159	Δ*cglB* + $cglB_{WT}$	TM913 $cglB_{WT}$ ($pCglB_{WT}$)	This work
TM1149	Δ*cglB* + $cglB_{D56A}$	TM913 $cglB_{D56A}$ ($pCglB_{D56A}$)	This work
TM1153	Δ*cglB* + $cglB_{S58A}$	TM913 $cglB_{S58A}$ ($pCglB_{S58A}$)	This work
TM1297	WT + *aglZ-mNeonGreen*	DZ2 pBJ*aglZ-mNeonGreen*	(*82*)
SI96	WT + IMss-mCherry	WT DZ2 transformed with plasmid pSWU19-PpilA-IMss-mCherry	This work
SI97	Δ*gltK* + IMss-mCherry	Δ*gltK* transformed with plasmid pSWU19-PpilA-IMss-mCherry	This work

SI98	Δ*gltB* + IMss-mCherry	Δ*gltB* transformed with plasmid pSWU19-PpilA-IMss-mCherry	This work
SI99	Δ*gltA* + IMss-mCherry	Δ*gltA* transformed with plasmid pSWU19-PpilA-IMss-mCherry	This work
SI100	Δ*gltH* + IMss-mCherry	Δ*gltH* transformed with plasmid pSWU19-PpilA-IMss-mCherry	This work

Table S2. *Myxococcus xanthus* strains used in this study.

Strain	**Genotype/Description**	**Source or Reference**
BL21(DE3)	*fhuA2* [lon] *ompT* gal *(λ DE3)* [dcm] Δ*hsdS* λ *DE3* = λ *sBamHIo* Δ*EcoRI-B* int::(*lacI*::P*lac*UV5::T7 gene1) i21 Δ*nin5*	Laboratory stock
DH5α	F-, Δ(argF-lac)U169, phoA, supE44, Δ(lacZ)M15, relA, endA, thi, hsdR	Laboratory stock

Table S3. *Escherichia coli* strains used in this study.

Plasmid	**Genotype/Description**	**Construction**	**Source or Reference**
pSWU30	Used for integration at phage Mx8 attB site (TetR)	/	Laboratory stock
pCglB$_{WT}$	pSWU30 with *cglB*	From pSWU30	This work
pCglB$_{D56A}$	pSWU30 with *cglB*$_{D56A}$	From pCglB$_{WT}$	This work
pCglB$_{S58A}$	pSWU30 with *cglB*$_{S58A}$	From pCglB$_{WT}$	This work
pSWU19-PpilA-IMss-mCherry	pSWU19 expressing IMss-mCherry under control of the *pilA* promotoer	From pSWU19	(*37*)
pBJ114	*galK*-containing vector for generation of in-frame deletions in *M. xanthus* (Kan^R)	/	Laboratory stock
pBJ*AglZ-YFP*	pBJ114 with a cassette allowing construction of the *aglZ-YFP* chimeric gene	From pBJ114	(*12*)
pBJΔ*gltK*	pBJ114 with a deletion cassette for *gltK*	From pBJ114	(*7*)
pBJΔ*gltB*	pBJ114 with a deletion cassette for *gltB*	From pBJ114	(*7*)
pBJΔ*gltA*	pBJ114 with a deletion cassette for *gltA*	From pBJ114	(*7*)
pBJΔ*gltBA*	pBJ114 with a deletion cassette for *gltBA*	From pBJ114	This work
pBJΔ*gltI*	pBJ114 with a deletion cassette for *gltI*	From pBJ114	(*7*)
pBJΔ*gltJ*	pBJ114 with a deletion cassette for *gltJ*	From pBJ114	(*11*)
pCDF-duet1	Expression vector, *lacI*, P*T7*, Streptomycin Resistant (Sm^R).	/	Novagen
pCDF-GltK^{6H}-BAC^S	*gltK*-6xHis into MCS1 , *gltBA and gltC*-StrepII into MCS2 cloned into pCDF-duet 1 (Sm^R).	From pCDF-duet1	This work
pET-duet1	Expression vector, *lacI*, P*T7*, Ampicillin Resitant (Amp^R).	/	Novagen
pET-GltH-CglB	*gltH* and *cglB* (*cglB* is inserted with a shine dalgarno sequence) cloned into pET-duet 1 MCS1 (AmpR).	From pET-duet1	This work

pACYC-duet1	Expression vector, *lacI*,P*T7*, Chloramphenicol Resistant (ChloR).	/	Novagen
pACYC-GltBAC^{S}	gltBA and gltC-StrepII into MCS2 cloned into pACYC-duet 1, (ChloR).	From pACYC-duet1	This work

Table S4. Plasmids used in this study.